



The effect of Tin addition on Structural and magnetic properties of the stannoferrite $\text{Li}_{0.5+0.5x}\text{Fe}_{2.5-1.5x}\text{Sn}_x\text{O}_4$

Y.M. Abbas, A. Hassan Ibrahim*, A. Bakry.M

Physics Department, Faculty of Science, Suez Canal University, Ismailia, 42111, Egypt

Ymabbas@gmail.com

ahmedphysics.ah@gmail.com

ABSTRACT

The physical properties of ferrites are very sensitive to microstructure, which in turn critically depends on the manufacturing process. Nanocrystalline Lithium Stannoferrite system $\text{Li}_{0.5+0.5x}\text{Fe}_{2.5-1.5x}\text{Sn}_x\text{O}_4$, $x = (0, 0.2, 0.4, 0.6, 0.8 \text{ and } 1.0)$ fine particles were successfully prepared by double sintering ceramic technique at pre-sintering temperature of 500°C for 3 h and the pre-sintered material was crushed and sintered finally in air at 1000°C . The structural and microstructural evolutions of the nanophase have been studied using X-ray powder diffraction (XRD) and the Rietveld method. The refinement results showed that the nanocrystalline ferrite has a two phases of ordered and disordered phases for polymorphous lithium Stannoferrite. The particle size of as obtained samples were found to be ~ 20 nm through TEM that increases up to ~ 85 nm and is independent on the annealing temperature. TEM micrograph reveals that the grains of the sample are spherical in shape. (TEM) analysis confirmed the X-ray results. The particle size of stannic substituted lithium ferrite fine particle obtained from the XRD using Scherrer equation. Magnetic measurements obtained from lake shore's vibrating sample magnetometer (VSM), saturation magnetization of ordered LiFe_5O_8 was found to be (57.829 emu/g) which was lower than disordered LiFe_5O_8 (62.848 emu/g). The interplay between superexchange interactions of Fe^{3+} ions at A and B sublattices gives rise to ferrimagnetic ordering of magnetic moments, with a high Curie-Weiss temperature ($T_{\text{CW}} \sim 900$ K).

Key words

Lithium Stannoferrite, Curie temperature, Ceramic technique, Polymorphism, Coercivity, Magnetization, Superparamagnetism, Rietveld, Fullprof.

Academic Discipline And Sub-Disciplines

Physics; Solid State Physics

SUBJECT CLASSIFICATION

Crystallographic study

TYPE (METHOD/APPROACH)

Experimental

INTRODUCTION

Lithium ferrites have been a widely investigated material due to its importance in both interesting properties and tremendous applications [1, 2]. New physical properties of ferrites and new technologies both in sample preparation and device fabrication on account of the development of nanoscience. Any change in cation distribution also results into an unexpected magnetic and electrical behaviour. Lithium iron oxides are promising candidates for cathode materials in rechargeable lithium batteries and also increasing scientific interest. A low-cost solid-state technique very suitable for the synthesis of nanocrystalline ferrite powders, exhibiting many of the desired properties [3–6].

The method of preparation, chemical composition, duration, annealing temperature, grain size and doping additives play an important role for tailoring the properties of spinel type ferrites for various applications.

Spinel-type LiFe_5O_8 is known to occur in two polymorphic modifications. The first one is a disordered β - LiFe_5O_8 [7] that obtained by the rapid quenching of the samples from high temperatures above 1000°C to room temperature; it has a disordered face centered cubic structure (space group $\text{Fd-}3\text{m}$, $a = 8.333 \text{ \AA}$). Under slow cooling, an order–disorder phase transition occurs near 750°C . This ordered inverse spinel phase, termed α - LiFe_5O_8 , with a primitive cubic unit cell (space group $\text{P}4_3\text{2}$, $a = 8.337 \text{ \AA}$) [8] this phenomena known as the polymorphism. Later, Schierer [9] discovered two other high temperature phases, and named them δ - LiFe_5O_8 (cubic, $a = 8.501 \text{ \AA}$), and γ - LiFe_5O_8 (tetragonal, $a = 6.025 \text{ \AA}$, $c = 7.534 \text{ \AA}$) which cannot be back to the previous two phases.

In the present study a double sintering ceramic technique was used for the synthesis of polycrystalline $\text{Li}_{0.5+0.5x}\text{Fe}_{2.5-1.5x}\text{Sn}_x\text{O}_4$, $x = (0, 0.2, 0.4, 0.6, 0.8, \text{ and } 1.0)$ powders. The single phase lithium Stannoferrite was characterized using XRD. Rietveld analysis [10–12] has been applied on the present study to determine the microstructural parameters of nano stannoferrite prepared system. The motivations of analysis are: (i) characterizing the nanoferrites in terms of microstructural parameters and (ii) estimating the distribution of cations among (A) and [B] sites in the crystal lattice.



EXPERIMENTAL DETAILS

1. Sample Preparation

The nanocrystalline single-phase $\text{Li}_{0.5+0.5x}\text{Fe}_{2.5-1.5x}\text{Sn}_x\text{O}_4$, ($x = 0, 0.2, 0.4, 0.6, 0.8, \text{ and } 1.0$) was synthesized by the standard ceramic technique. The initial materials were Li_2CO_3 (Sigma-Aldrich, 99 wt%) and $\alpha\text{-Fe}_2\text{O}_3$ (Alfa Aesar, 88 wt%), SnO_2 (Alfa Aesar, 99.9 wt%). The powders were first hand ground in an agate mortar in a wet medium (acetone) for 1 h to get a homogeneous mixture and then the samples were dried at 200°C , ground manually and pre-calculated in high purity alumina crucibles at 500°C for 3 h in the open air. Then the powder was pressed in a disk-shaped form of 13-mm diameter, and 3- to 5-mm thickness. The pre calcinated mixtures were divided into two sections; the first section was fired to 1000°C for 9 h, then dropped in the crashed ice. Then remilled mechanically again, for else 10 min to get the disordered phase of the stannoferrite system, the second section was finally sintered to 1000°C for 9 h, then cooled slowly down to the room temperature then remilled again for else 10 min to get the ordered phase of the stannoferrite system.

2. Characterization of Samples

Phase analysis of lithium stannoferrite samples was investigated by X-ray diffractometer, XRD, employing Cu K α radiation ($\lambda = 1.540560 \text{ \AA}$) (type X'Pert pro panalytical Diffractometer) at the Agricultural Centre of Research (ACR) (Giza, Egypt). The XRD patterns were recorded at room temperature in 2θ range of 10° – 90° and a scanning rate of $2^\circ (2\theta) / \text{min}$. To correct instrumental broadening a LaB_6 standard [13] was used. The particle size of the samples was calculated using the Sherrer's relation.

The particle morphology was examined by transmission electron microscope TEM (Philips, EM400) at Petroleum Centre of Research (PCR), Nasr City, Egypt, and the Vibrating sample magnetometer (VSM) is used for the magnetic measurement (model 7310, lake shore) at the agricultural center of researches (ACR), El-Dokki, Egypt.

3. Rietveld Analysis of the Experimental Data [10–12]

3.1. Method of Analysis

The FullProf program has been mainly developed for Rietveld analysis (structure profile refinement) of neutron (constant wavelength, time of flight, nuclear and magnetic scattering) or X-ray powder diffraction data collected at a constant or variable step in scattering angle 2θ . The program can be also used as a Profile Matching (or pattern decomposition using the Le Bail method) tool, without the knowledge of the structure. Single crystal refinement can also be performed alone or in combination with powder data.

The shape of the peaks in the experimental diffraction patterns was well described by Thompson-Cox-Hastings pseudo-Voigt convoluted with an axial divergence asymmetry function which provide a good approximation to most peaks. To simulate the theoretical X-ray powder diffraction patterns of the stannoferrite system, the following considerations for the different phases were made:

- 1- Identification of the phases by computer search-match to compare the experimental pattern with the International Centre for Diffraction Data (ICDD) database of known compounds.
- 2- Index the diffraction pattern to determine the crystal system, unit cell dimensions and space group.

3.2. Crystal Structure Refinement

A detailed calculations of the mathematical procedures implemented in the Rietveld analysis have been reported elsewhere [14–20]. The progress of the minimization the difference between the observed and calculated powder diffraction patterns was described through the reliability parameters, R_{wp} (weighted residual factor), and R_{exp} (expected residual factor) defined as:

$$R_{wp} = \left[\frac{\sum_i w_i (I_o - I_c)^2}{\sum_i w_i (I_o)^2} \right]^{1/2}$$
$$R_{exp} = \left[\frac{N - P}{\sum_i w_i (I_o)^2} \right]^{1/2}$$

Where I_o and I_c are the experimental and calculated intensities, $w_i = 1/I_o$ are weight factors, N is the number of experimental observations and P is the number of refined parameters. Goodness of fit (GoF) factor defined as the ratio of weighted to expected residual factor [17–21]:

$$GoF = \frac{R_{wp}}{R_{exp}}$$

Refinements were repeated with much more iterations until convergence was reached and the value of the GoF factor became close to 1.

4. Results and discussion

4.1. XRD Analysis

The X-ray diffraction patterns of the two polymorphous α - $\text{Li}_{0.5}\text{Fe}_{2.5}\text{O}_4$ and β - $\text{Li}_{0.5}\text{Fe}_{2.5}\text{O}_4$ are shown in Fig (1). X-ray diffraction analysis by computer search matching for the polymorph LiFe_5O_8 showed that samples consisted of single phase and they do not contain any reflection from starting phases, It is observed that the peak corresponding to the planes (311), (440), (511) and (220) confirming the phase formation of pure disordered β - LiFe_5O_8 with a well defined spinel structure of space group "Fd-3m" without any impure phase and the peak corresponding to the planes (110), (210) and (211) confirming the phase formation of pure ordered α - LiFe_5O_8 with a well defined cubic structure of space group "P4₃32" without any impure phase and coinciding with the (ICCD:04-007-9427).

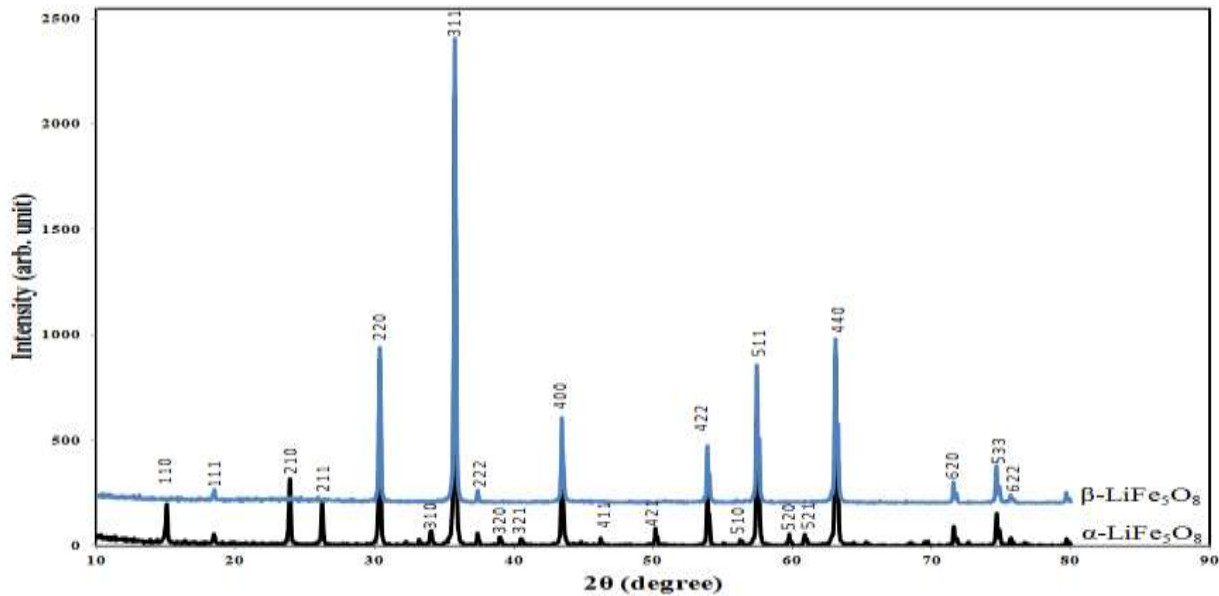


Figure (1) X-ray diffraction pattern for α - LiFe_5O_8 and β - LiFe_5O_8 prepared systems.

Figure (2.a) and Figure (2.b) represents the X-ray diffraction patterns of the two polymorphous $\text{Li}_{0.5+0.5x}\text{Fe}_{2.5-1.5x}\text{Sn}_x\text{O}_4$ ($x = 0.0, 0.2$ and 0.4), which were confirmed to be cubic structure of space groups "Fd-3m" and "P4₃32" for each of disordered and ordered phases respectively.

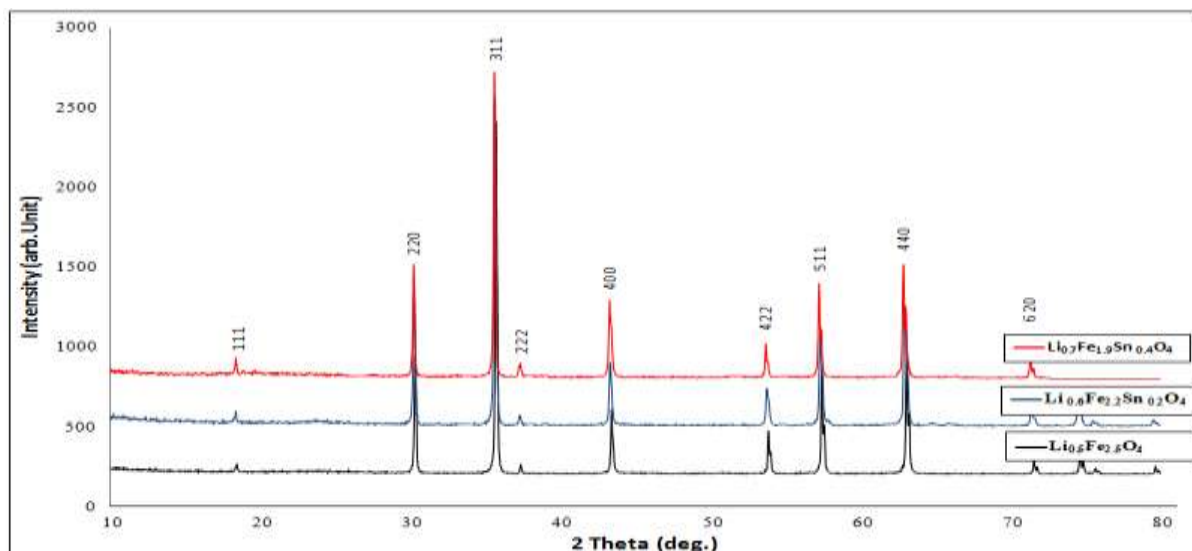


Figure (2.a) X-ray diffraction pattern for disordered $\text{Li}_{0.5+0.5x}\text{Fe}_{2.5-1.5x}\text{Sn}_x\text{O}_4$ ($x=0.0, 0.2$ and 0.4) of space group 'Fd-3m'.

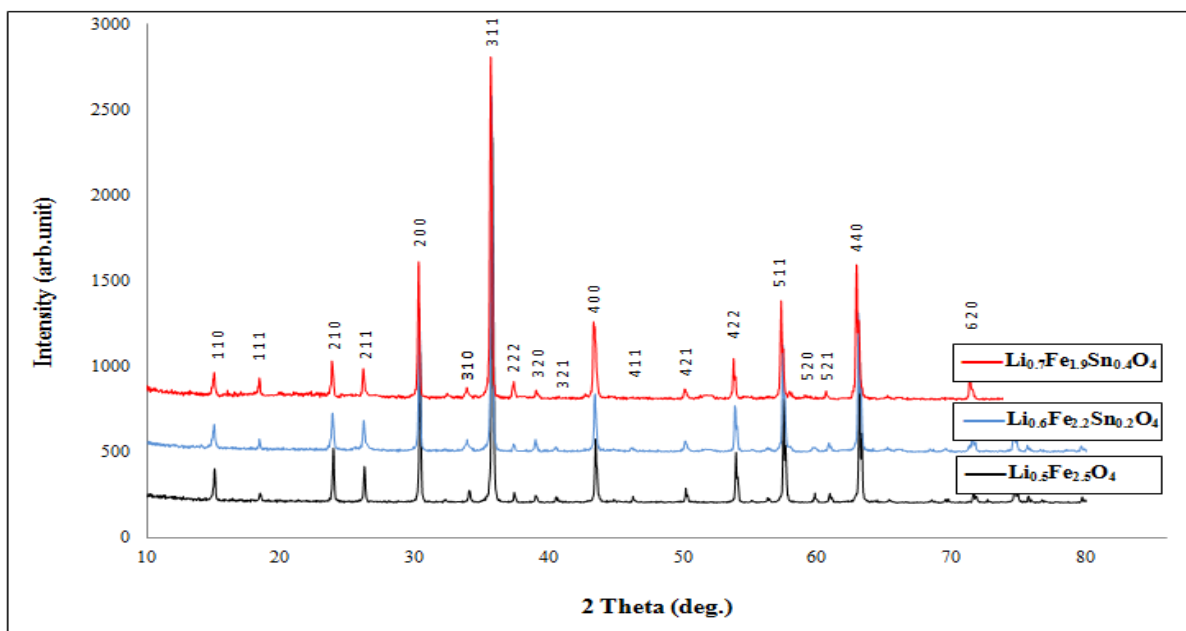


Figure (2.b) X-ray diffraction pattern for ordered $\text{Li}_{0.5+0.5x}\text{Fe}_{2.5-1.5x}\text{Sn}_x\text{O}_4$ ($x=0.0, 0.2$ and 0.4) of space group 'P4₃32'

On the other hand, from the x-ray diffraction data, we found a new polymorph by increasing the Sn^{4+} content in ferrite system $\text{Li}_{0.5+0.5x}\text{Fe}_{2.5-1.5x}\text{Sn}_x\text{O}_4$ ($x > 0.4$). X-ray diffraction analysis by computer search matching for the new polymorph $\text{Li}_{0.5+0.5x}\text{Fe}_{2.5-1.5x}\text{Sn}_x\text{O}_4$ ($x=0.6, 0.8$ and 1.0) in disordered phase with a well defined orthorhombic structure of space group "P m c n" without any impure phase, and coinciding with the (COD: 96-100-1220)[22], And in ordered phase with a well defined hexagonal close packed structure of space group "P 63 mc" without any impure phase, and coinciding with the (COD:96-100-0435) [23].

Figure (3.a) and Figure (3.b) represents the X-ray diffraction patterns of the two polymorphous $\text{Li}_{0.5+0.5x}\text{Fe}_{2.5-1.5x}\text{Sn}_x\text{O}_4$ ($x=0.6, 0.8$ and 1.0). The X-ray diffraction analysis by computer search matching for nanocrystalline Polymorphs $\text{Li}_{0.5+0.5x}\text{Fe}_{2.5-1.5x}\text{Sn}_x\text{O}_4$ ($x = 0.6, 0.8$ and 1.0) showed that all samples consisted of single phase and do not contain any reflection from starting phases, which were confirmed to be orthorhombic and hexagonal close packed structure of space groups "P m c n" and "P 63 mc" for each of disordered and ordered phases respectively.

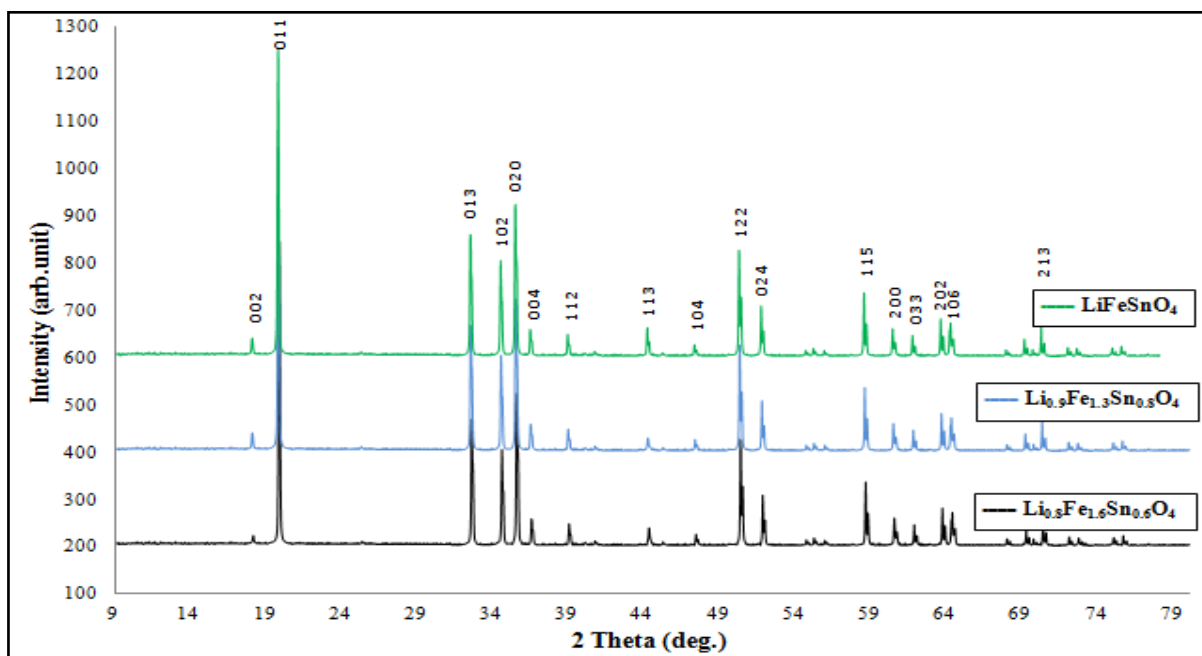


Figure (3.a) X-ray diffraction pattern for orthorhombic structure $\text{Li}_{0.5+0.5x}\text{Fe}_{2.5-1.5x}\text{Sn}_x\text{O}_4$ ($x=0.6, 0.8$ and 1.0) of space group 'P m c n'.

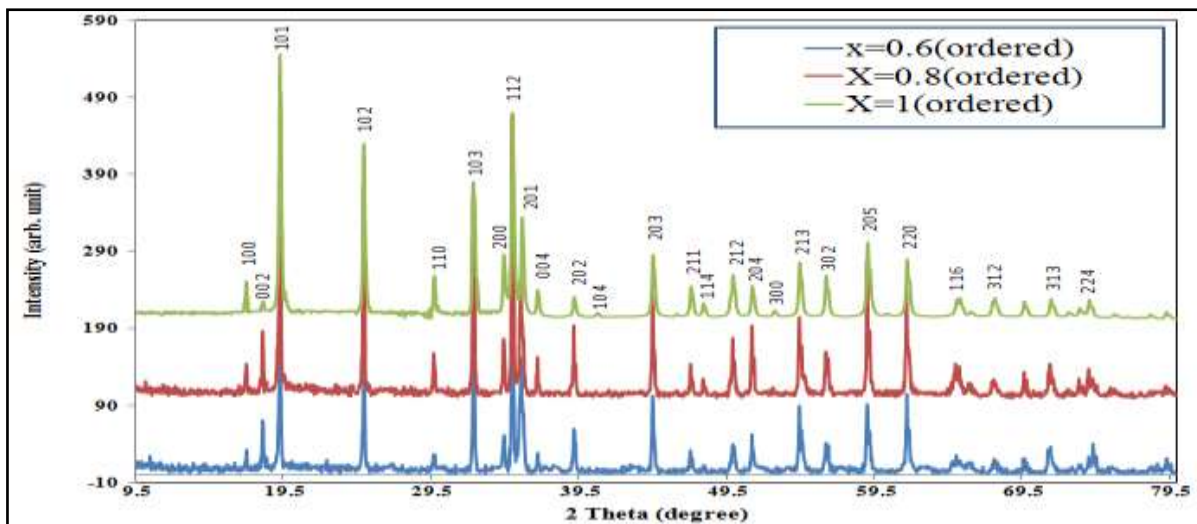


Figure (3.b) X-ray diffraction pattern for double hexagonal close packed $\text{Li}_{0.5+0.5x}\text{Fe}_{2.5-1.5x}\text{Sn}_x\text{O}_4$ ($x = 0.6, 0.8$ and 1.0) of space group 'P 63 mc'.

4.2. Refinement of XRD data

FULLPROF Rietveld software has been used for XRD data. Refinements were performed in space groups: (Fd-3m), (P4₃32), (P m c n) and (P 63 ms) for different polymorphic stannoferrite systems. Atomic scattering factor for fully ionized atoms Li^{1+} , Fe^{3+} , Sn^{4+} and O^{2-} were taken from the international table for crystallography volume C (1992).

In each refinement, a total of more than twenty parameters were refined: zero shift, scale factor, background coefficients, three lattice constants, asymmetry parameter, three oxygen parameters for isotropic temperature factor, and parameter for the full width at half maximum.

The Rietveld plots of the refinements for different polymorphic lithium stannoferrite $\text{Li}_{0.5+0.5x}\text{Fe}_{2.5-1.5x}\text{Sn}_x\text{O}_4$ ($x=0.0$ and 1.0) are given in figures (4.a to 4.d).

Figures (5.a) and (5.b) zooms out a part of the pattern of the profile fitting for each of the two polymorphic $\text{Li}_{0.5}\text{Fe}_{2.5}\text{O}_4$ prepared system to indicate the agreement between the observed and calculated data.

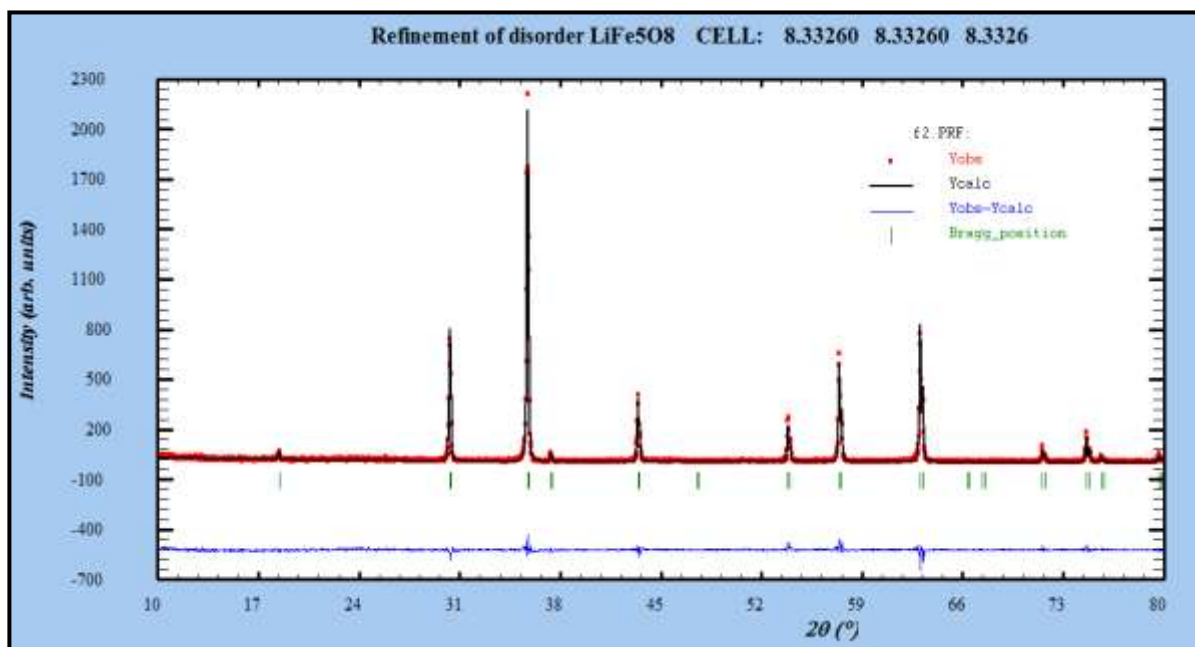


Figure (4.a) The profile fitting for disordered $\text{Li}_{0.5}\text{Fe}_{2.5}\text{O}_4$, with a well defined face centred cubic structure of space group "Fd-3m".

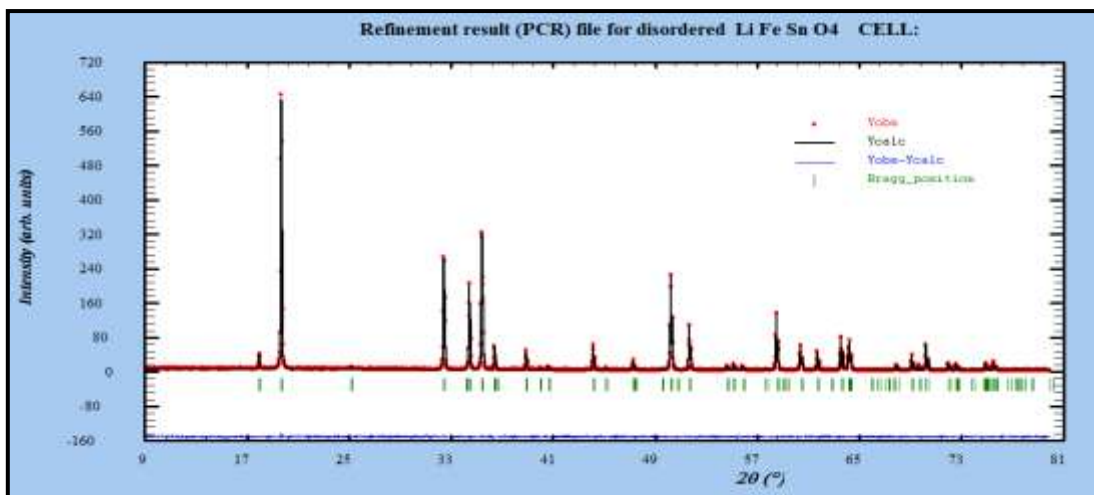


Figure (4.b) The profile fitting disordered phase LiFeSnO_4 , with a well defined orthorhombic structure of space group “P m c n”.

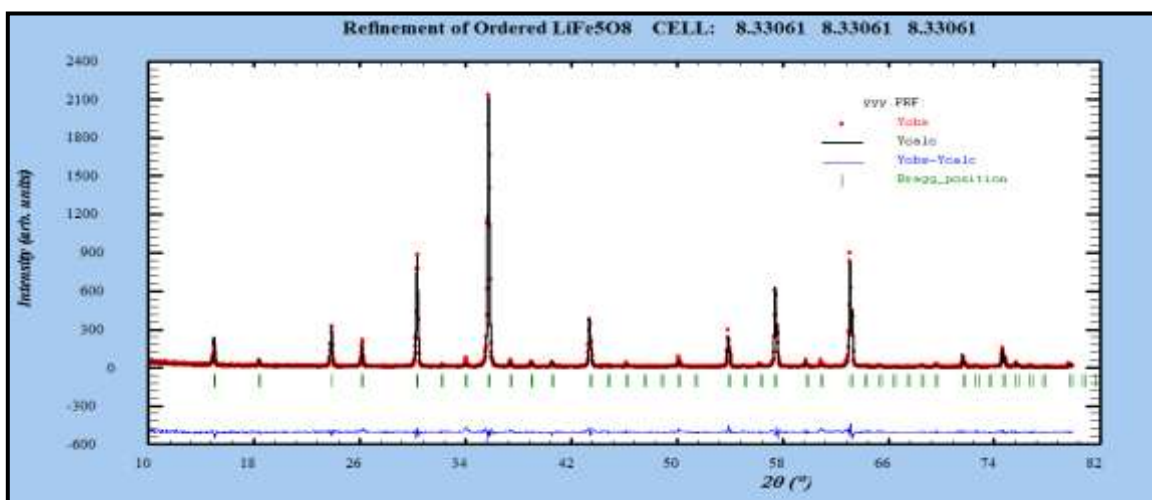


Figure (4.c) The profile fitting for ordered phase $\text{Li}_{0.5}\text{Fe}_{2.5}\text{O}_4$, with a well defined primitive cubic structure of space group “P4₃32”.

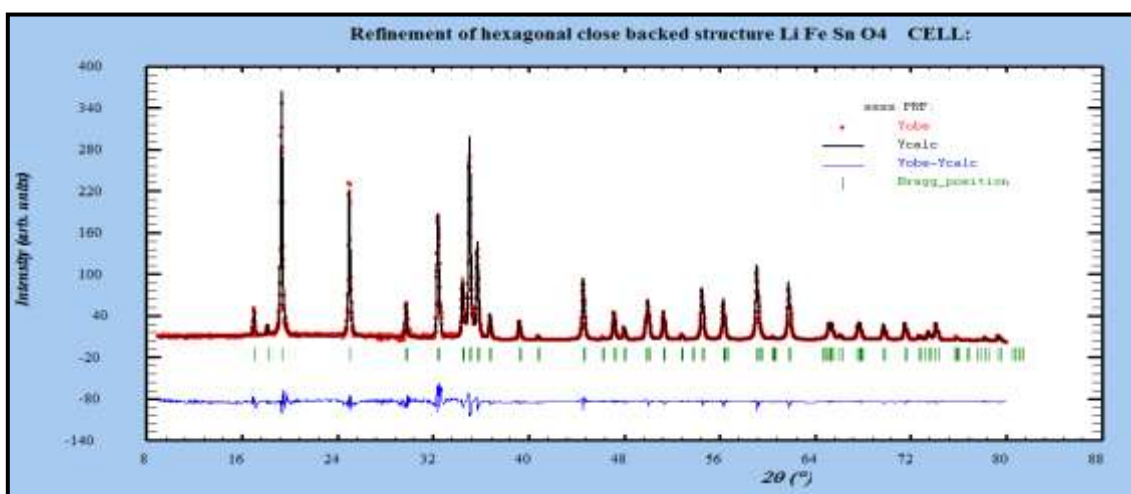


Figure (4.d) The profile fitting for double hexagonal close packed LiFeSnO_4 , of space group “P 63 mc”.

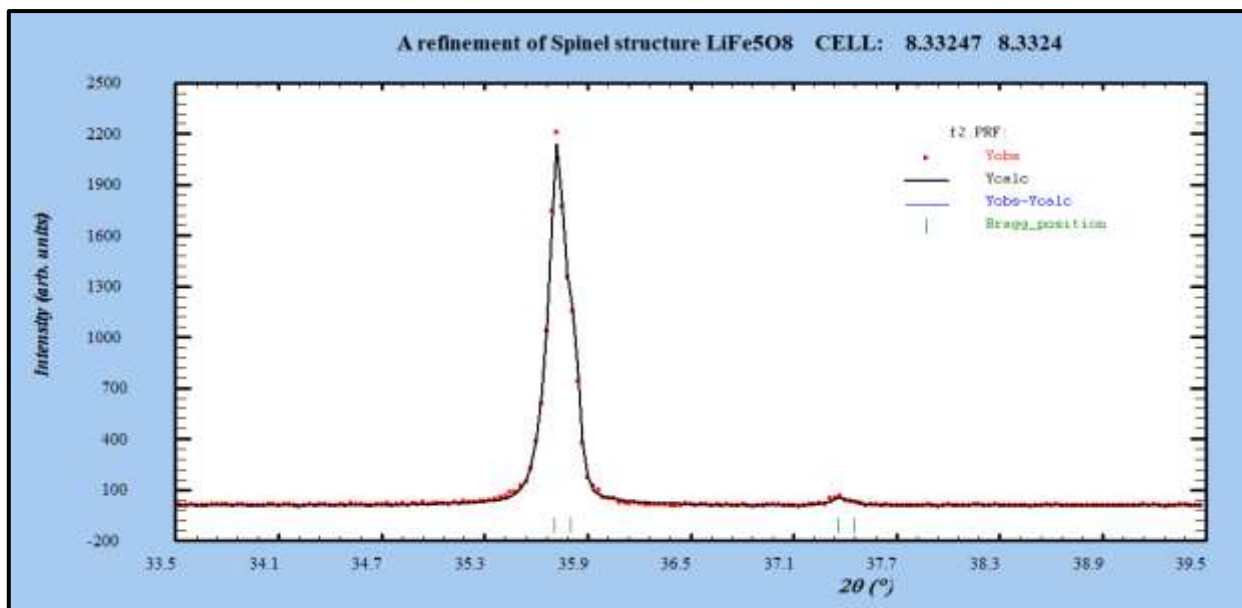


Figure (5.a) Zoom out of a part of the pattern of the profile fitting for disordered $\text{Li}_{0.5}\text{Fe}_{2.5}\text{O}_4$

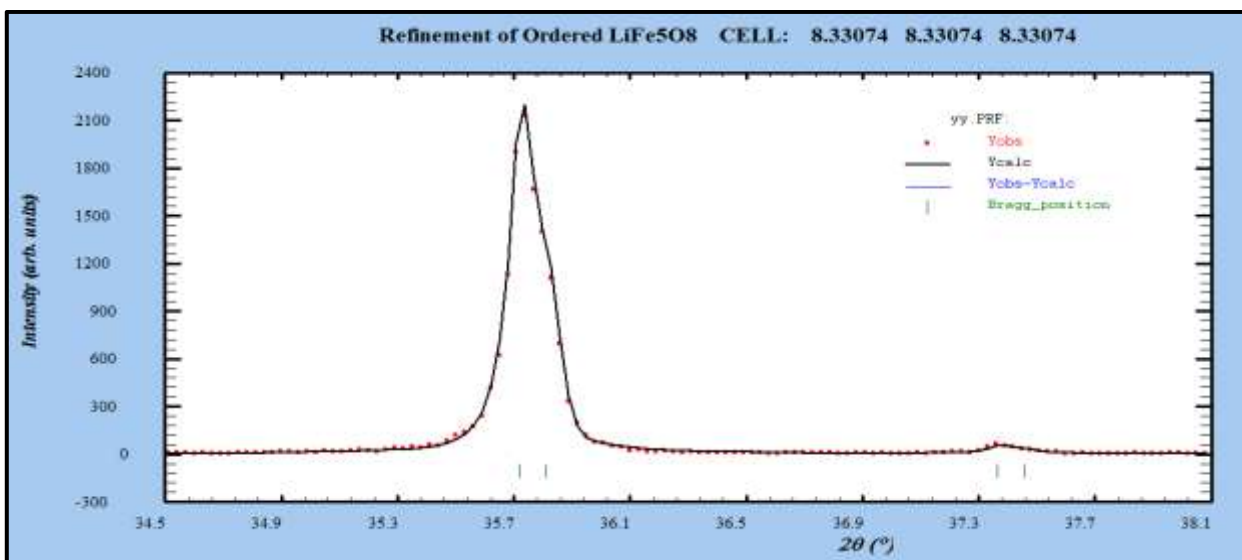


Figure (5.b): Zoom out of a part of the pattern of the profile fitting for ordered $\text{Li}_{0.5}\text{Fe}_{2.5}\text{O}_4$

The lattice parameter a (Å), oxygen parameter U , and fitting parameters of the two polymorphic modifications of the Stannoferrite system $\text{Li}_{0.5+0.5x}\text{Fe}_{2.5-1.5x}\text{Sn}_x\text{O}_4$ are displayed in table (1).

Table (1): The lattice parameter a (Å), oxygen parameter U , and fitting parameters of the two polymorphic modifications of the Stannoferrite $\text{Li}_{0.5+0.5x}\text{Fe}_{2.5-1.5x}\text{Sn}_x\text{O}_4$.

Phase	Composition	Crystal structure	GoF	Bragg R-factor	RF- Factor	a (Å)	b (Å)	c (Å)	U
Disordered system	$\text{Li}_{0.5}\text{Fe}_{2.5}\text{O}_4$		1.2252	5.259	4.245	8.332612	-	-	0.019018
	$\text{Li}_{0.6}\text{Fe}_{2.2}\text{Sn}_{0.2}\text{O}_4$	Cubic	1.2892	5.755	5.024	8.341465	-	-	0.014811
	$\text{Li}_{0.7}\text{Fe}_{1.9}\text{Sn}_{0.4}\text{O}_4$		'Fd-3m'	1.2904	8.123	7.428	8.351823	-	-
	$\text{Li}_{0.8}\text{Fe}_{1.6}\text{Sn}_{0.6}\text{O}_4$	orthorhombic	0.9998	3.760	4.882	3.065272	5.068636	9.87318	0.520000
	$\text{Li}_{0.9}\text{Fe}_{1.3}\text{Sn}_{0.8}\text{O}_4$		1.0010	1.725	3.675	3.064236	5.066195	9.87318	0.530000
	LiFeSnO_4	'P m c n'	1.0120	3.974	2.416	3.064219	5.066166	9.86935	0.520000



Ordered system	$\text{Li}_{0.5}\text{Fe}_{2.5}\text{O}_4$	Cubic 'P4 ₃ 32'	1.2880	7.468	7.953	8.330613	-	-	0.420322
	$\text{Li}_{0.6}\text{Fe}_{2.2}\text{Sn}_{0.2}\text{O}_4$		1.7432	8.301	8.42	8.333716	-	-	0.415838
	$\text{Li}_{0.7}\text{Fe}_{1.9}\text{Sn}_{0.4}\text{O}_4$		1.8200	8.532	8.023	8.350012	-	-	0.424230
	$\text{Li}_{0.8}\text{Fe}_{1.6}\text{Sn}_{0.6}\text{O}_4$	DH 'P63mc'	0.9990	3.182	2.129	6.000912	-	9.76636	0.264114
	$\text{Li}_{0.9}\text{Fe}_{1.3}\text{Sn}_{0.8}\text{O}_4$		1.0021	3.924	2.291	6.00102	-	9.76724	0.263000
	LiFeSnO_4		1.1000	4.002	2.427	6.002046	-	9.76830	0.25630

4.2.1 Cations Distribution

In the ordered form (space group P4₁32/P4₃32) the Fe³⁺ ions are at octahedral 12d and tetrahedral 8c sites, and Li⁺ ions occupy only the octahedral 4b positions in the cubic primitive unit cell. The disordered LiFe₅O₈ has an inverse spinel structure (space group Fd-3m), with Fe³⁺ at tetrahedral 8a positions and Li⁺ and Fe³⁺ randomly distributed over the 16d octahedral sites. The order-disorder transition in the lithium ferrite structure may be recorded by the X-ray diffraction. Relations between the (Fd3m) and (P4₃32) Wyckoff's positions are as follows [24]:

Fd-3m → P4₃32

8a (8 Fe³⁺) 8c (8 Fe³⁺)

16d (12 Fe³⁺ + 4 Li⁺) 12d (12 Fe³⁺) + 4b (4 Li⁺)

32e (32 O²⁻) 24e (24 O²⁻) + 18c (8 O²⁻)

It is well known that the magnetic properties of spinel ferrites depend on the summation of the magnetic moments at (A) and [B] sites [25]. It has been also experimentally verified that the cation distributions among the lattice sites depends on the preparation technique. Cation distributions on A-site and B-site for the two ferrite systems are shown in table (2).

Table (2): Cation distribution on (A-site) and [B-site] for both prepared systems.

Composition	Cation distribution (A-site)	Cation distribution [B-site]	Cation distribution (A-site)	Cation distribution [B-site]
	Disordered system		Ordered system	
$\text{Li}_{0.5}\text{Fe}_{2.5}\text{O}_4$	(Li _{0.01250} Fe _{0.98746})	[Li _{0.50046} Fe _{1.49954}]	(Fe _{0.33333})	[Li _{0.16666} Fe _{0.50000}]
$\text{Li}_{0.6}\text{Fe}_{2.2}\text{Sn}_{0.2}\text{O}_4$	(Li _{0.01999} Fe _{0.98752})	[Li _{0.48800} Sn _{0.2010} Fe _{1.44462}]	(Sn _{0.02283} Fe _{0.32123})	[Li _{0.18530} Sn _{0.04383} Fe _{0.43754}]
$\text{Li}_{0.7}\text{Fe}_{1.9}\text{Sn}_{0.4}\text{O}_4$	(Li _{0.02933} Fe _{0.97067})	[Li _{0.47500} Sn _{0.4001} Fe _{1.12500}]	(Sn _{0.04225} Fe _{0.29108})	[Li _{0.18500} Sn _{0.09108} Fe _{0.39028}]
$\text{Li}_{0.8}\text{Fe}_{1.6}\text{Sn}_{0.6}\text{O}_4$	(Li _{0.07531})	[Li _{0.167060} Sn _{0.1500} Fe _{0.3500}]	-	-
$\text{Li}_{0.9}\text{Fe}_{1.3}\text{Sn}_{0.8}\text{O}_4$	(Li _{0.07843})	[Li _{0.17157} Sn _{0.19550} Fe _{0.3250}]	-	-
LiFeSnO_4	(Li _{0.07532})	[Li _{0.17572} Sn _{0.2500} Fe _{0.25000}]	-	-

The refinement result showed that the nanocrystalline ferrite phase is partially an inverse spinel. The information of mixed spinel instead of inverse spinel may result due to the decrease in the occupancy of Fe³⁺ cation on (A) site during the formation of spinel ferrite. At the same time, the occupancy of Li¹⁺ cation on [B] site decreases and then increases on (A) site. This occurs when there is a random distribution of cations among the (A) and [B] sites inside the spinel matrix.

The refinement result showed that the Cation distributions on tetrahedral and octahedral sites for double hexagonal close packed LiFeSnO₄ was confirmed to be (Li_{0.56}Fe_{0.42}) T1 (Li_{1.00}) T2 (Sn_{1.00}) oc1 (Sn_{0.9993}Li_{0.4398}Fe_{1.56}) oc2 O₈, tin is only located at only the octahedral sites, while iron and lithium are distributed on both tetrahedral sites and octahedral sites of the framework structure. On the other hand the distribution of cations on tetrahedral and octahedral sites for orthorhombic LiFeSnO₄ of space group 'P m c n' was confirmed to be (Li_{0.30128}) T (Li_{0.70288}Sn_{1.00}Fe_{1.00}) oct O₄, (~30%) of lithium ions occupy the (T) tetrahedral site, and (~70%) occupy the (oc) site. Tin cation Sn⁴⁺ occupy the octahedral site with a preferential occupancy of (oc) site, and iron Fe³⁺ cation occupy the octahedral site.



4.2.2. Inter Atomic Distance and the Inter Bond Angles

The inter atomic distance between the cations on the tetrahedral (A) and octahedral [B] sites has been calculated with the help of the following relations [26]:

$$M_A - M_A = \left(\frac{\sqrt{3}}{4}\right) a \quad M_A - M_B = \left(\frac{\sqrt{\pi}}{4}\right) a$$

$$M_B - M_B = \left(\frac{\sqrt{2}}{4}\right) a \quad M_A - O_A = a\sqrt{3}(\delta + 1/8)$$

$$M_B - O_B = a \left(\frac{1}{16} - \frac{\delta}{2} + 3\delta^2\right)^{1/2}$$

Where δ is a deviation from oxygen parameter (U) and $\delta = U - U_{ideal}$ and $R_0 =$ radius of oxygen ion = 1.35 Å [27].

These parameters are important to give a full description of the crystal structure, and connection with the magnetic properties. Where M_A and M_B refer to the cations at the center of the tetrahedral (A) and octahedral [B] sites respectively, while O_A and O_B refer to the center of an oxygen anion, related to the tetrahedral (A) and octahedral [B] configuration respectively. The calculated values of these distances for ordered and disordered $Li_{0.5+0.5x}Fe_{2.5-1.5x}Sn_xO_4$, ($x=0.0, 0.2$ and 0.4) are listed in table (3).

Table (3): The calculated values of inter-atomic distance between the cations on the tetrahedral (A-site) and octahedral (B-site) for the two cubic systems of space group 'Fd-3m' and 'P4₃32'.

Composition	C. Structure/ space group	$M_A - M_A$	$M_A - M_B$	$M_B - M_B$	$M_A - O_A$	$M_B - O_B$
Li_{0.5}Fe_{2.5}O₄	Cubic	3.608066	3.6922309	2.945974	1.886661	2.0534616
Li_{0.6}Fe_{2.2}Sn_{0.2}O₄	'Fd-3m'	3.6119602	3.69621544	2.949153	1.902500	2.0605283
Li_{0.7}Fe_{1.9}Sn_{0.4}O₄		3.6164454	3.70080521	2.952815	1.920562	2.0642832
Li_{0.5}Fe_{2.5}O₄	Cubic	3.607261	3.6914067	2.94532	1.86355	2.056325
Li_{0.6}Fe_{2.2}Sn_{0.2}O₄	'P4 ₃ 32'	3.6086048	3.6927817	2.94613	1.89589	2.062033
Li_{0.7}Fe_{1.9}Sn_{0.4}O₄		3.6156612	3.7000027	2.95217	1.91000	2.0700024

4.2.3. Microstructure Analysis

The main aims of analysis to characterize the material in terms of microstructural parameters such as crystallite size and root mean square (r.m.s.) lattice strain. The average crystallite size and lattice strain for both disordered and ordered prepared systems are shown in table (4).

Table (4): Average crystallite and lattice strain for both ordered and disordered polymorphous systems.

Chemical Composition	Disordered prepared system		Ordered prepared system	
	Average crystallite size (nm)	Lattice strain	Average crystallite size (nm)	Lattice strain
Li_{0.5}Fe_{2.5}O₄	51.8375	0.3367%	32.256	0.3012%
Li_{0.6}Fe_{2.2}Sn_{0.2}O₄	39.8625	0.2095%	30.564	0.2156%
Li_{0.7}Fe_{1.9}Sn_{0.4}O₄	43.5263	0.1610%	30.025	0.1542%
Li_{0.8}Fe_{1.6}Sn_{0.6}O₄	36.5266	0.1856%	34.545	0.2431%
Li_{0.9}Fe_{1.3}Sn_{0.8}O₄	44.2560	0.2103%	40.542	0.2805%
LiFeSnO₄	75.2145	0.2547%	92.954	0.2852%

4.3. Transmission Electron Microscopy (TEM)

Transmission electron microscopy (TEM) is considered the main method for characterizing the microstructure of nanocrystalline materials [28]. TEM micrograph showed that the particles of sample are spherical in shape and the average crystallite size between (25-85) nm as shown in Figs.6 and 7, which is quite closer to the X-ray crystallite size calculations. However, some particles are quite bigger due to crystallite size growth of small grains of spinel phase and variation of density of it clearly corroborate the findings. The non uniform particle size distribution should attribute to a non-uniform ingredient mixture and a non-uniform grain distribution of powder.

The Microstructure of the disordered prepared samples $\text{Li}_{0.5}\text{Fe}_{2.5}\text{O}_4$, $\text{Li}_{0.7}\text{Fe}_{1.9}\text{Sn}_{0.4}\text{O}_4$ and LiFeSnO_4 samples have been characterized by TEM micrograph as shown in figures (6.a to 6.c). On the other hand TEM micrograph for ordered $\text{Li}_{0.5}\text{Fe}_{2.5}\text{O}_4$ and (DH) LiFeSnO_4 samples are shown in figures (7.a) and (7.b).

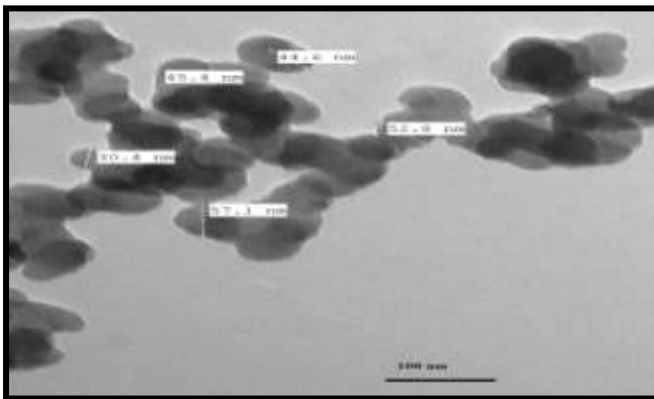


Figure (6.a): TEM micrograph for disordered $\text{Li}_{0.5}\text{Fe}_{2.5}\text{O}_4$.

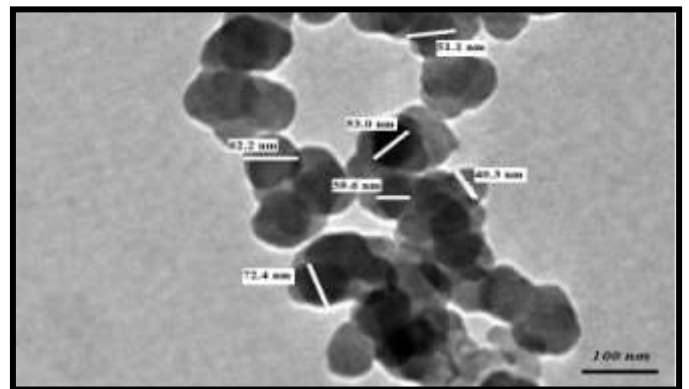


Figure (6.b): TEM micrograph for disordered $\text{Li}_{0.7}\text{Fe}_{1.9}\text{Sn}_{0.4}\text{O}_4$.

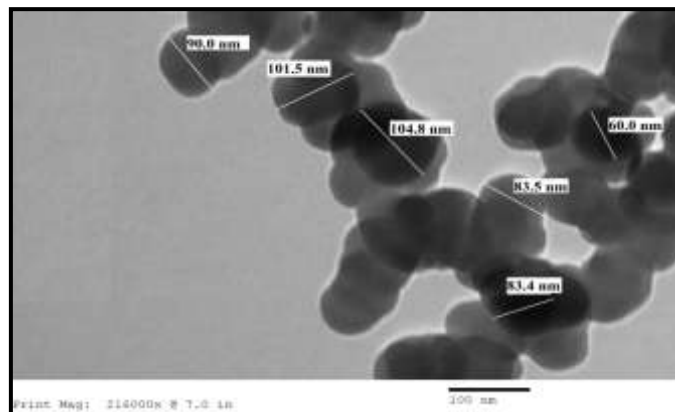


Figure (6.c): TEM micrograph for ordered $\text{Li}_{0.5}\text{Fe}_{2.5}\text{O}_4$.

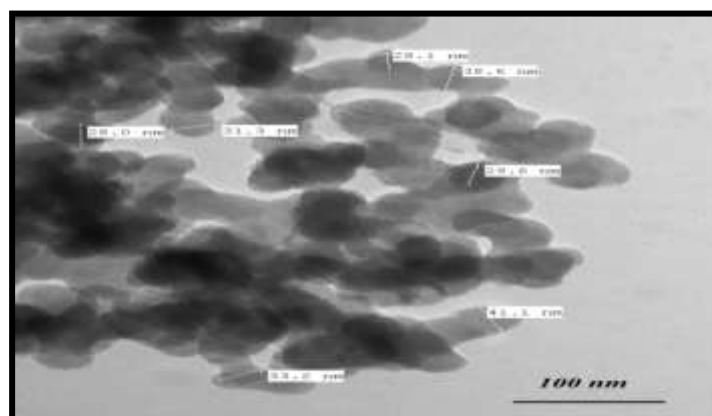


Figure (7.a): TEM micrograph for double hexagonal close packed LiFeSnO_4 .

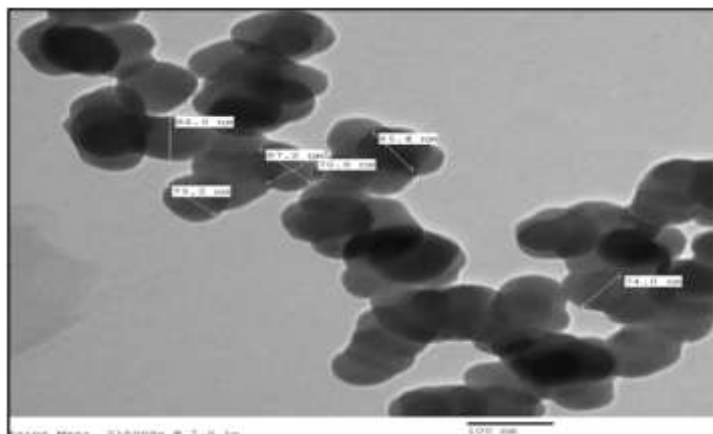


Figure (7.b): TEM micrograph for orthorhombic LiFeSnO_4

4.4 Magnetic Measurements

Vibrating Sample Magnetometer (VSM)

The magnetic hysteresis loops were characterized to determine parameters, such as the saturation magnetization (M_s), remnant magnetization (M_r) and coercivity (H_c). The magnetic properties of powders have been determined at room temperature using a vibrating sample magnetometer in the maximum external field of 20 KOe.

The hysteresis loops for the disordered and ordered nanocrystalline $\text{Li}_{0.5+0.5x}\text{Fe}_{2.5-1.5x}\text{Sn}_x\text{O}_4$, ($x=0.0, 0.2, 0.4, 0.6, 0.8$ and 1.0) are shown in (Fig.8) and (Fig.9) respectively; the hysteresis loop for the nanocrystalline lithium Stannoferrite samples show the superparamagnetic behaviour, with value of magnetic susceptibility $\sim 0.0045-0.0049$, the difference in the saturation magnetization in the two systems due to the difference in cation distribution at the tetrahedral and octahedral sites [29]. Since H_c is very small and approximately approach to zero comparing to the applied field, the as obtained samples for polymorphous systems exhibits no hysteresis, which may be attributed to superparamagnetic relaxation as confirmed by XRD.

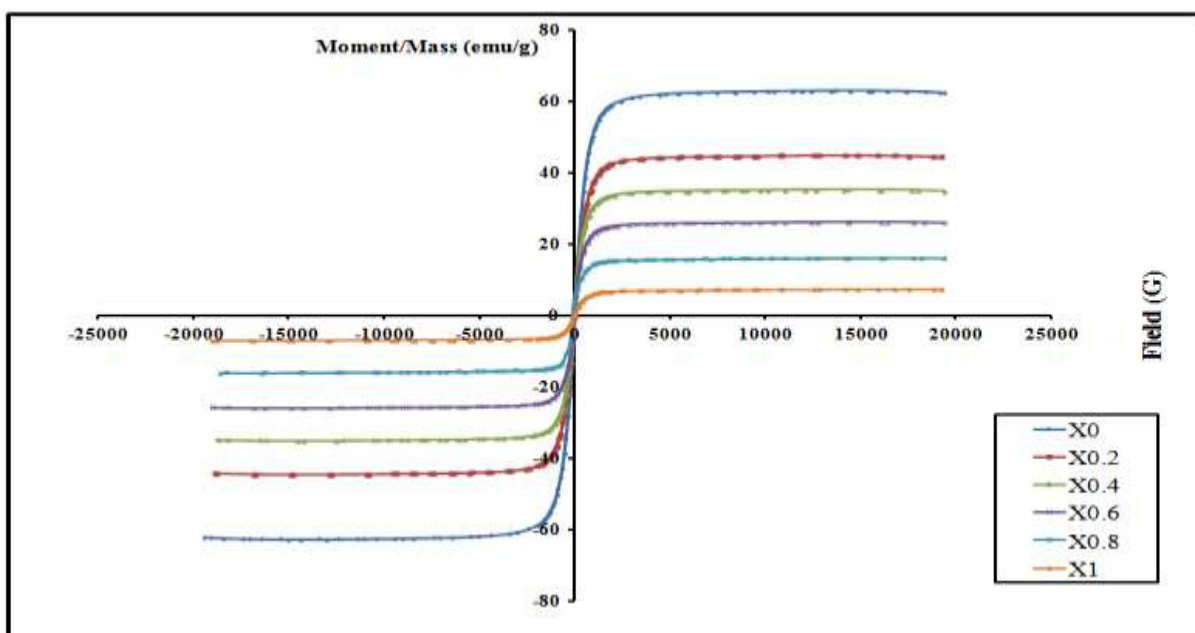


Figure (8): Superparamagnetism in disordered $\text{Li}_{0.5+0.5x}\text{Fe}_{2.5-1.5x}\text{Sn}_x\text{O}_4$ prepared systems, X0, X0.2, X0.4, X0.6, X0.8, X1, refer respectively to ($X=0.0, 0.2, 0.4, 0.6, 0.8$ and 1.0).

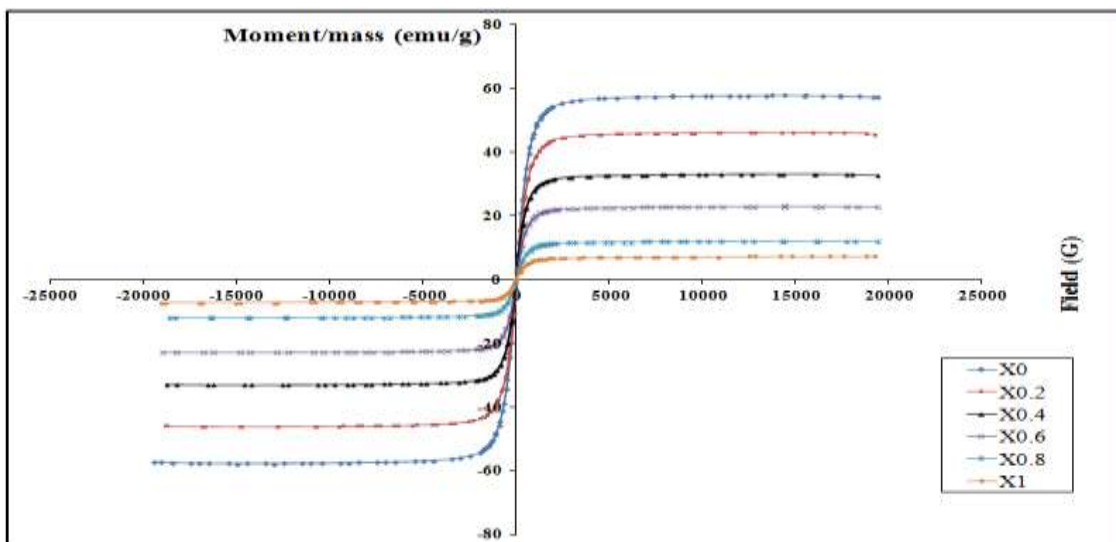


Figure (9): Superparamagnetism in ordered polymorphs $\text{Li}_{0.5+0.5x}\text{Fe}_{2.5-1.5x}\text{Sn}_x\text{O}_4$ prepared systems, X0,X0.2,X0.4, X0.6, X0.8, X1, refer respectively to (X=0.0, 0.2, 0.4 , 0.6, 0.8 and 1.0).

Magnetization of the polymorphous system $\text{Li}_{0.5}\text{Fe}_{2.5}\text{O}_4$ decreases monotonically with raising temperature, as shown in (Fig.10), the Curie temperature of the pure $\text{Li}_{0.5}\text{Fe}_{2.5}\text{O}_4$ is equal to 900 K; the decreases in magnetization and Curie temperature are caused by structural and magnetic disorder in spin like surface layer of nanograins.

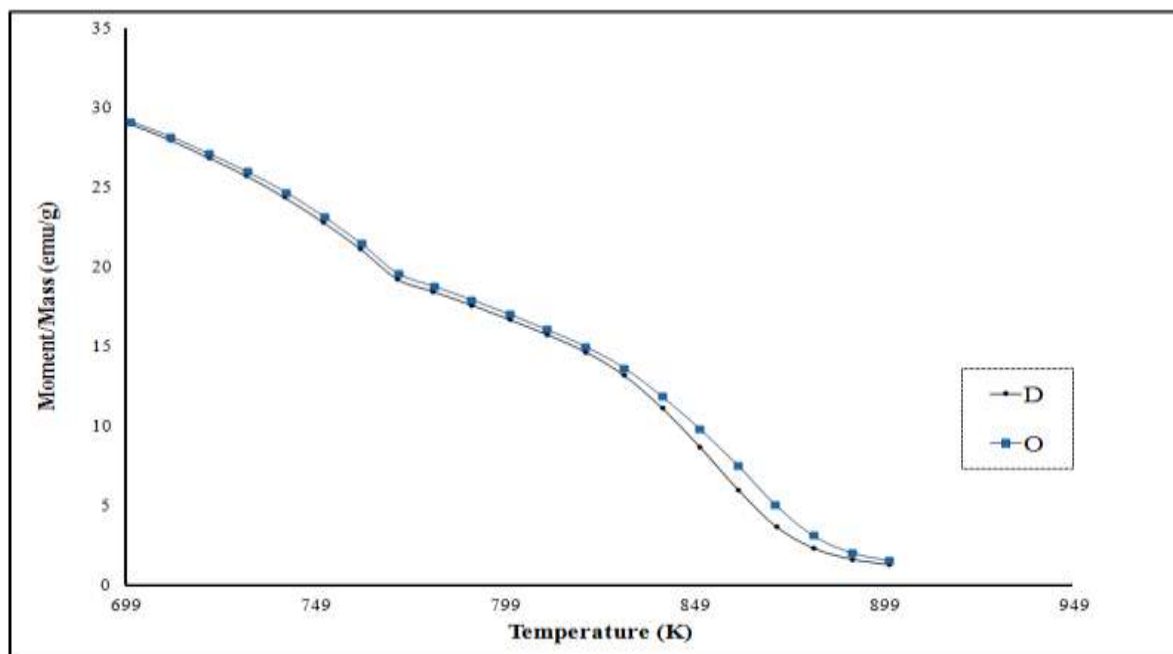


Figure (10): Temperature variation of magnetization for the two polymorphous $\text{Li}_{0.5}\text{Fe}_{2.5}\text{O}_4$

From table (5) we note that the saturation magnetization of ordered LiFe_5O_8 was found to be (57.829 emu/g). This was lower than disordered LiFe_5O_8 (62.848 emu/g) [30]. This behaviour is attributed to the nature of disordered surface effects of the small particles [31, 32] which appear as a result of the finite size of nanocrystallites and which lead to a non-collinearity of the magnetic moments at the nanocrystallites surface. These effects are getting more intense when the mean size of the nanocrystallites is getting smaller. The decrease in saturation magnetization with decreasing particle size has been illustrated by Morrish [33]. The decrease of the saturation magnetization in the case of nanoparticles systems was also observed by other authors [34, 35]. This proves that a magnetic behaviour is related to the variation of the particle size.



Table (5): Magnetic parameters obtained from magnetization curves for the two polymorphous systems.

Chemical composition	System	Hc (G)	Ms(emu/g)	Mr(emu/g)	R=Mr/Ms	χ_m	μ_r	Average crystalline size (nm)
$\text{Li}_{0.5}\text{Fe}_{2.5}\text{O}_4$	Disordered System	6.569	62.848	1.47510	0.02347091	0.0049	1.0049	51.8375
$\text{Li}_{0.6}\text{Fe}_{2.2}\text{Sn}_{0.2}\text{O}_4$		4.016	44.713	0.92911	0.02077942	0.0039	1.0039	39.8625
$\text{Li}_{0.7}\text{Fe}_{1.9}\text{Sn}_{0.4}\text{O}_4$		3.002	35.0198	0.84350	0.02408630	0.0025	1.0025	43.5263
$\text{Li}_{0.8}\text{Fe}_{1.6}\text{Sn}_{0.6}\text{O}_4$		2.512	25.9050	0.62059	0.02395637	0.0013	1.0013	36.5266
$\text{Li}_{0.9}\text{Fe}_{1.3}\text{Sn}_{0.8}\text{O}_4$		3.001	15.9444	0.45690	0.02865582	0.0083	1.0083	44.2560
LiFeSnO_4		13.201	7.9002	0.25641	0.03245614	0.0007	1.0007	75.2145
$\text{Li}_{0.5}\text{Fe}_{2.5}\text{O}_4$	Ordered system	5.675	57.839	1.2229	0.02114317	0.0045	1.0045	32.256
$\text{Li}_{0.6}\text{Fe}_{2.2}\text{Sn}_{0.2}\text{O}_4$		6.870	46.176	1.4010	0.03034043	0.0040	1.0040	30.564
$\text{Li}_{0.7}\text{Fe}_{1.9}\text{Sn}_{0.4}\text{O}_4$		12.244	33.129	1.5612	0.0169398	0.0029	1.0029	30.025
$\text{Li}_{0.8}\text{Fe}_{1.6}\text{Sn}_{0.6}\text{O}_4$		13.412	22.987	0.98952	0.04304690	0.0020	1.0020	34.545
$\text{Li}_{0.9}\text{Fe}_{1.3}\text{Sn}_{0.8}\text{O}_4$		11.758	12.124	0.50060	0.04129000	0.0011	1.0011	40.542
LiFeSnO_4		12.202	7.3222	0.24991	0.03413045	0.0006	1.0006	92.954

The values of calculated and observed magnetic moment of the two polymorphous $\text{Li}_{0.5}\text{Fe}_{2.5}\text{O}_4$ displayed in a table (6). The calculated magnetic moments for disordered and ordered prepared systems are shown in table (7) and (8) respectively.

Table (6): The values of calculated and observed a magnetic moment for the two polymorphic LiFe_5O_8 .

Crystal structure	M_S	$n_B(\mu_B)$	
	(emu/gm)	Obs.	Cal
$\beta\text{-LiFe}_5\text{O}_8$	62.848	2.33030	2.50000
$\alpha\text{-LiFe}_5\text{O}_8$	57.839	2.81162	2.79980

Table (7): The magnetic moment of tetrahedral (A-site) and octahedral (B-site) for disordered prepared system.

Composition	$M_A(\mu_B)$	$M_B(\mu_B)$	μ (molecule)
$\text{Li}_{0.5}\text{Fe}_{2.5}\text{O}_4$	4.78730	7.44770	2.66040
$\text{Li}_{0.6}\text{Fe}_{2.2}\text{Sn}_{0.2}\text{O}_4$	4.93760	7.22310	2.28550
$\text{Li}_{0.8}\text{Fe}_{1.6}\text{Sn}_{0.6}\text{O}_4$	0.00000	1.75000	1.75000
$\text{Li}_{0.9}\text{Fe}_{1.3}\text{Sn}_{0.8}\text{O}_4$	0.00000	1.62500	1.62500
LiFeSnO_4	0.00000	1.25000	1.25000

Table (8): The magnetic moment of tetrahedral (A-site) and octahedral (B-site) for ordered prepared system.

Composition	$M_A(\mu_B)$	$M_B(\mu_B)$	μ (molecule)
$\text{Li}_{0.5}\text{Fe}_{2.5}\text{O}_4$	1.66665	2.50000	0.83335
$\text{Li}_{0.6}\text{Fe}_{2.2}\text{Sn}_{0.2}\text{O}_4$	1.60615	2.18770	0.58155
$\text{Li}_{0.7}\text{Fe}_{1.9}\text{Sn}_{0.4}\text{O}_4$	1.45540	1.95140	0.49600



5. CONCLUSION

- The conventional way of preparing the polycrystalline ferrite is by solid-state reaction, which involves the mixing of oxides with intermittent grinding followed by high temperature sintering at 1000 °C has been successfully used for the preparation of mixed nanosize spinel ferrites.
- The refinement result showed that the nanocrystalline $\text{Li}_{0.5+0.5x}\text{Fe}_{2.5-1.5x}\text{Sn}_x\text{O}_4$, ($x=0, 0.2$ and 0.4). The other samples of orthorhombic structure, ($x=0.6, 0.8$ and 1.0) instead of inverse spinel due to the presence of part of Li^{1+} cation on (A) site and the other part of Li^{1+} cation occupy [B] site with Sn^{4+} and iron Fe^{3+} cations, the occupancy of Fe^{3+} cation on [B] site increases and occupancy of Li^{1+} cation on [B] site decrease with increasing Sn^{4+} cation on [B] site. At the same time, in the inverse spinel system, the occupancy of Li^{1+} on [B] site decreases and then increase on (A) site. On the other hand the occupancy of Fe^{3+} cation decreases on [B] site and increase on (A) site. This occurs when there is a random distribution of cations among the (A) and [B] sites inside the spinel matrix.
- The refinement results showed that the nanocrystalline ferrite has a two phases of disordered and ordered phases for polymorphous lithium Stannoferrite. This ordered phase, termed $\alpha\text{-LiFe}_5\text{O}_8$, with a primitive cubic unit cell (space group $P4_332$). On the other hand, from the x-ray diffraction data, we found a new polymorph by increasing the Sn^{4+} content in ferrite system $\text{Li}_{0.5+0.5x}\text{Fe}_{2.5-1.5x}\text{Sn}_x\text{O}_4$ ($x>0.4$) prepared samples.
- TEM micrograph reveals that the grains of samples are spherical in shape and the average size of the particles is between (25-85) nm which is quite closer to the X-ray crystallite size. However, some of the particles are quite bigger due to the crystallite size growth of small grains and variation in density of grains clearly corroborates the findings.
- The hysteresis loops were measured to determine parameters, such as the saturation magnetization (M_s), remnant magnetization (M_r), and coercivity (H_c).
- From magnetic measurement we found that:
 - 1) The magnetic properties of the samples clearly depend on the size of the nanocrystallites.
 - 2) The magnetic properties of a spinel ferrite, are strongly dependent on the distribution of the different cations among [A] and [B] sites.
 - 3) The decrease in saturation magnetization (M_s) can be attributed to decrease of the mean size of nanocrystallites.
 - 4) The coercive force (H_c) is size dependent.
 - Our results for nanocrystalline $\text{Li}_{0.5+0.5x}\text{Fe}_{2.5-1.5x}\text{Sn}_x\text{O}_4$ prepared system show that the H_c is very small and approximately approach to zero comparing to the applied field, the as obtained samples for polymorphous systems exhibits no hysteresis, which may be attributed to superparamagnetic relaxation as confirmed by XRD.
 - Magnetization of the two polymorphous systems $\text{Li}_{0.5}\text{Fe}_{2.5}\text{O}_4$ decreases monotonically with raising temperature and the Curie temperature of the pure $\text{Li}_{0.5}\text{Fe}_{2.5}\text{O}_4$ is equal to 900 K.

REFERENCES

- I. H.J. Ritcher, J. Appl. Phys. 32 ,R147(1999).
- II. H. Gleiter, J.Weissmuller, O.Wollersheim, R.Wurschum, Acta Mater. 49, 737(2001).
- III. P. Druska, U. Steinike, V. Sepelak, J. Solid State Chem. 146, 13(1999).
- IV. V. Sepelak, A.Yu. Rogachev, U. Steinike, D.Chr. Uccker, S. Wibmann, K.D. Becker, Acta Crystallogr. A 52 (Suppl.) 367, (1996).
- V. V. Sepelak, K. Tkacova, V.V. Boldyrev, U. Steinike, Mater. Sci. Forum 783, 228(1996).
- VI. V. Sepelak, A.Yu. Rogachev, U. Steinike, D.Chr. Uccker, F. Krumcich, S. Wibmann, K.D. Becker, Mater. Sci. Forum 139, 235(1997).
- VII. M. Kiyama, T. Takeda, Bull. Inst. Chem. Res. Kyoto Univ. 58, 193(1980).
- VIII. J.L. Dorman, M. Nogue, Acta Crystallogr. C 39, 1615 (1983).
- IX. M. Schierer, J. Inorg. Nucl. Chem. 26, 1363(1964).
- X. N.W. Grimes, R.J. Hilleard, J. Waters, J. Yerkess, J. Phys. C (Prog. Phys. Soc.) 1 663(1968).
- XI. G. Blasse, Philips Res. Rep. Suppl. 3 91(1964).
- XII. G.E. Bacon, F.F. Roberts, Acta Crystallogr. 6 57 (1953).
- XIII. M.Zhang, L.Yuan, X. Wang, H.Fan, X.Wang, X.Wu, H.Wang, Y. Qian, Journal of Solid State Chemistry 181 (2), 294-297 (2008).



- XIV. H.M. Rietveld, Acta Crystallogr. 22 151(1967).
XV. H.M. Rietveld, J. Appl. Crystallogr. 2 65(1969).
XVI. L. Lutterotti, MAUDWEB, Version 1.9992, 2004. <http://www.ing.unitn.it/~luttero/maud>.
XVII. S. Bid, S.K. Pradhan, J. Appl. Crystallogr. 35 517 (2002).
XVIII. S. Bid, S.K. Pradhan, Mater. Chem. Phys. 82 27(2003).
XIX. H. Dutta, S.K. Manik, S.K. Pradhan, J. Appl. Crystallogr. 36 260 (2003).
XX. S.K. Manik, S.K. Pradhan, Mater. Chem. Phys. 86 2284 (2004).
XXI. H. P. Klug and L. E. Alexander, "X-ray diffraction procedures for poly crystalline and amorphous materials," Second Edition, Wiley, (1974).
XXII. P.Lacorre, M.Hervieu, J.Pannetier, J.Choisnet, B.Raveau, Journal of Solid State Chemistry 50, 196-203 (1983).
XXIII. J. Choisnet, M. Hervieu, B.Raveau, Tarte P, "Two Polymorphous Lithium Stannoferrites Li FeSnO₄: A Ramsdellite- Type and a Hexagonal Close-Packed Structure", Journal of Solid State Chemistry 40, 344-351 (1981).
XXIV. A. Tomas, P. Laruelle, J. L. Dormann, Nogues M. Acta Crystallogr.C39, 1615-1617 (1983).
XXV. S.K. Pradhan, S. Bidb, M. Gateshki, V. Petkov, Material Chimestry and Physics 93,224 (2005).
XXVI. K.J. Standley, Oxide Magnetic Materials, Oxford University Press, London, p 64 (1962).
XXVII. J. Smit, Magnetic properties of materials, McGrawHill Book Company New York, (1971).
XXVIII. R. Grössinger, G. Badurek, J.Fidler, M. Zehetbauer, C.D. Dewhurst, Journal of Magnetism and Magnetic Materials 294,152(2005).
XXIX. Y.M. Abbas, S.A. Mansour, M.H. Ibrahim, Shehab.E. Ali, Journal of Magnetism and Magnetic Materials 324, 2781-2787 (2012).
XXX. V. Pillai, D.O. Shah, Journal of Magnetism and Magnetic Materials 163, 243-248 (1996).
XXXI. R.H. Kodama, A.E. Berkowitz, S. Foner, Phys. Rev. Lett.77, 394(1996).
XXXII. C. Caizer, Journal of Magnetism and Magnetic Materials 251, 304 (2002).
XXXIII. A.H. Morrish, K. Haneda, J. Appl. Phys. 52, 2496(1981).
XXXIV. A. S. Albuquerque, J. D. Ardisson, W. A. A. Macedo, Journal of Magnetism and Magnetic Materials, 192, 277 (1999).
XXXV. P. Mollard, P. Germi, A. Rousset Physica B+C, Volumes 86-88, Part3, 1393-1394 (1977).

Author' biography

Yehiamohammed Abbas

Professor of solid state physics, Suez Canal University

E.mail: Ymabbas@gmail.com

Cell phone: +2(010)09996969

Ahmed Hassan Ibrahim

Ph.D. student, assistant lecturer, physics department, Suez Canal University

E..mail: ahmedphysics.ah@gmail.com

Cell phone: +2(012)82564204

Ahmed Bakry Mansour Elaydy

Lecturer of physics, Suez Canal University

